USGS Earthquake Hazards Program Award G16AP00034: Final technical report

Mapping the extents of creep on the faults of the northern San Francisco Bay Area using repeating earthquakes

Gareth Funning and Nader Shakibay Senobari, University of California, Riverside

Principal investigator: Gareth Funning
University of California
Department of Earth Sciences
900 University Ave
Riverside, CA 92521
Telephone: 951-827-2037
Fax: 951-827-4324
E-mail: gareth@ucr.edu

Term covered by the award: 03/01/2016–02/28/2017

Abstract

The aim of this project is to map the extent of creep on the major strike-slip faults in the northern San Francisco Bay Area using the locations of repeating earthquake sequences, which are considered indicators of creep. Creep, which can reduce the seismic hazard posed by faults, has previously been observed on the Rodgers Creek, Maacama and Bartlett Springs faults, but due to issues of access and geodetic data coverage, we do not have a complete picture of the distribution of creep on these faults; geodetic data also have limited resolution with depth.

We use a multi-step approach to identify and verify repeating earthquake sequences. First, we cross-correlate all event waveforms on a station-by-station basis within sub areas of our region of interest and retain pairs of events with cross-correlation coefficients > 0.9. Next, we cluster the events that are highly correlated at multiple stations and use a hierarchical clustering algorithm to identify events with high similarity. We then use differential S-P times, estimated by a cross-spectral approach, and precise relative relocations to confirm that our candidate repeating earthquake sequences have overlapping source radii.

We find in total 96 repeating earthquake ‘families’ and 91 repeating earthquake pairs. The Maacama fault has a repeating earthquake distribution that is consistent with pervasive creep along its full length, and exhibits significant structural complexity at its northern and southern ends, with subparallel active strands in both locations. The Rodgers Creek fault results are consistent with coherent creep to a depth of 7 km, along a segment northwest of Santa Rosa where we observe creep geodetically. At Lake Pillsbury, we find repeating events that suggest that the Bartlett Springs fault creeps over its full seismogenic width.

USGS Earthquake Hazards Program Award G16AP00034: Final technical report

Mapping the extents of creep on the faults of the northern San Francisco Bay Area using repeating earthquakes

Gareth Funning and Nader Shakibay Senobari, University of California, Riverside

1. Introduction

The aim of this project is to map the extent of creep on the major strike-slip faults in the northern San Francisco Bay Area using the locations of repeating earthquake sequences, which are considered indicators of creep. Creeping faults accumulate less elastic strain than faults that are locked and undergo stick-slip behavior; furthermore, areas of creep may also act as barriers to seismic rupture. More accurate determinations of areas of fault creep will, in turn, lead to more accurate assessments of seismic hazard; in addition this information is important for investigating possible geological causes of creep.

1.1 Repeating earthquakes

We define repeating earthquakes (REs) as sequences of events which are quasi-periodic in occurrence and almost identical in terms of their waveforms and source characteristics (e.g. locations, magnitudes, mechanisms). They are typically identified by examining the similarity of waveforms from different earthquakes recorded at the same stations; a high degree of similarity implies that all the events in a RE sequence have the same source characteristics and the same location, and the seismic waves follow the same path. REs can also be identified through precise relative relocation methods (e.g. Vidale et al., 1994; Schaff and Beroza, 2004) if it can be demonstrated that the is likely to be a high degree of overlap between the rupture areas of successive events.

Most previous studies (e.g. Ellsworth and Dietz, 1990; Nadeau and Johnson, 1998; Nadeau and McEvilly, 1999; Chen et al., 2007) interpret quasi-periodic REs as the result of recurrent rupture on a small locked patch on a fault surrounded by, and repeatedly loaded to failure by, a larger area of creep. The implication is that any detection of REs along a fault is a signature of the creep at depth on that fault. In addition, REs can be used for locating faults and determining their geometries at depth, and can help to elucidate complex fault zone structure.

1.2 The northern San Francisco Bay Area

Our area of interest in this study is the northern San Francisco Bay Area (hereafter, ‘North Bay’), a region dominated tectonically by major strike-slip fault systems, such as the San Andreas, Rodgers Creek–Maacama and Green Valley–Hunting Creek–Bartlett Springs faults (Figure 1).

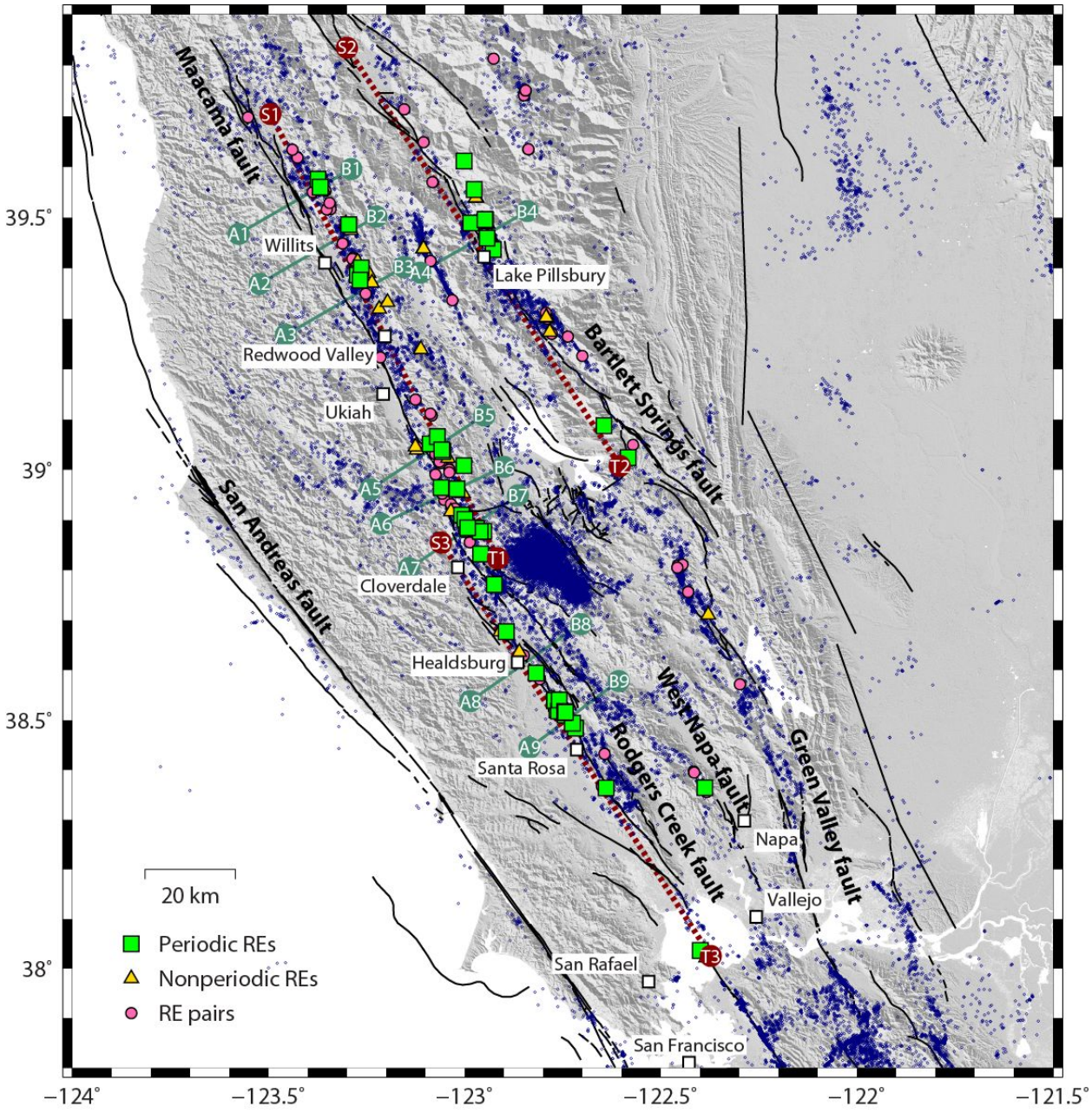

Figure 1: Seismicity, fault and repeating earthquake (RE) families in the northern San Francisco Bay Area. The majority of the periodic REs (green squares), nonperiodic REs (yellow triangles) and RE pairs (pink circles) are focused along the Rodgers Creek, Maacama and Bartlett Springs faults, indicating that these faults are likely to be creeping along much of their lengths. Locations of cross-fault (A-B; sea green) and along-strike (S-T; dark red) profiles corresponding to Figure 6 are marked. Relocated seismicity, from the near-real time double difference catalog for northern California (Waldhauser, 2009) is plotted as dark blue open circles.

We target in particular faults on which some surface observations of creep have been made, such as the Rodgers Creek, Maacama, Bartlett Springs, Green Valley and West Napa faults

(e.g. Harsh et al., 1978; Funning et al., 2007; Murray et al., 2014; McFarland et al., 2016; Jin and Funning, 2017). The major fault systems in the area are thought to be capable of destructive earthquakes that could threaten local and regional populations (e.g. Field et al., 2014), and our knowledge of the details of fault movement and strain accumulation for each is far less certain than for analogous structures further south in California. Most recently, the West Napa fault, the source of the M6.0 2014 South Napa earthquake, showed rapid and laterally extensive shallow creep in the month that followed in amounts, in some areas that equalled the maximum coseismic surface slip (e.g. Hudnut et al., 2014; Floyd et al., 2016). The South Napa event served as a reminder that partially-creeping faults present an ongoing seismic hazard, and that the creep – which caused repeat damage to some lifelines repaired in the immediate aftermath of the earthquake – can pose a hazard in its own right.

1.3 Detecting repeating earthquakes: methods and challenges

The most common method for detecting REs is by computing cross-correlation coefficients (CCCs), a measure of waveform similarity, between pairs of earthquakes, where a value of 1 indicates identical waveforms, and a value of 0 indicates zero similarity. By defining an appropriate CCC threshold, events that are highly similar, and thus are candidates to be REs can be identified.

There are two main challenges for detecting REs using CCC thresholding: i) False positives, i.e. incorrectly classifying groups of events as REs. This can result from a loss of diagnostic features in event waveforms due to attenuation or filtering – e.g. closely spaced, but not identical, events detected at distant stations can have high CCCs, and be incorrectly associated as REs. In such cases, defining a high CCC threshold, using higher frequency bandpass filters or excluding stations based upon distance might be a way to decrease false positives. ii) False negatives, i.e. incorrectly classifying REs as not repeating events. This can result from perturbations to waveforms, for example from station noise, temporal changes in the crust (e.g. Poupinet et al., 1984, Schaff et al., 2004), and/or differences in rupture propagation from event to event. These issues can be mitigated through defining a lower CCC threshold or using a lower frequency bandpass filter. Given that the solutions to the two challenges are, in effect, opposites, care must be taken in the selection of CCC thresholds, and, ideally, additional information should be used in the RE selection process.

One possible source of additional information is from precise earthquake locations. In this case, we would classify events as REs if the rupture areas of a pair of events overlap by some percentages (e.g. 50 percent; Waldhauser and Ellsworth, 2000). This method is potentially more robust but it requires the precise relocating of all events – potentially a large and unnecessary effort if the only goal is detection of REs.

To address both the challenges of false positives and negatives in RE detection, as well as the computational demand required to relocate events, we adopt a multi-stage approach in this study, in which a pool of candidate events are selected using a moderately high

cross-correlation threshold, and then validated by estimating first differential S–P arrival times, and then using these times to estimate precise relative event relocations. We apply these methods to local network waveform data from long-lived seismic stations.

2. Data

2.1 Data selection and retrieval

We divide the North Bay study area into 16 subregions, on average 30 × 50 km in dimension, each centered on a fault of interest (Figure 2). We base our subregion selection on the number of events within an area; for reasons of computational efficiency we aim for 6000 events or fewer. We allow for overlap of up to 10 km between subregions to ensure no repeating event families were missed at the edges. We then retrieve event and station information from the Northern California Earthquake Data Center (NCEDC) for the events within each subregion at the stations located inside these subregions and at distances up to 60 km outside their edges.

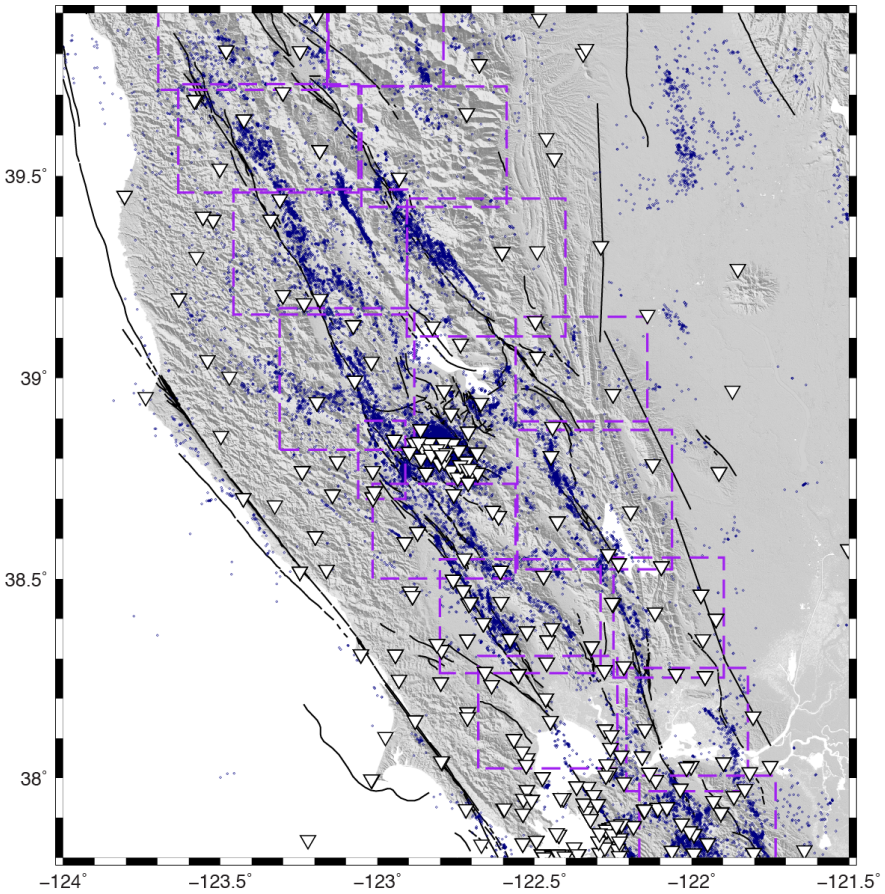

Figure 2: Seismic stations and earthquake subregions used in data selection. Over 43,000 events (dark blue circles) in 16 subregions (purple dashed boxes), detected at over 300 stations (white triangles) were used.

We include a station in our event search if two criteria are met: i) it has a duration of operation longer than 10 years; ii) it has detected over 100 events or more in the target subregion. For subregions with good station coverage (e.g. >150 stations with 100 detected events or more) we raise these thresholds to 15 years and 500 events, respectively. Our final station selections for each subregion range from a minimum of 10 stations to a maximum of 104, with the southernmost subregions typically covered by the greater numbers of stations.

Considering each subregion in turn and using phase arrival information from the Northern California Seismic Network (NCSN) catalog, we retrieve 20 seconds of waveform data from the NCEDC archive for each detected event at each station, starting 5 seconds before the P arrival and 15 seconds after. We use *IrisFetch.m* (Reyes and Karstens, 2014) for this data retrieval. This window size is based on the small sizes (i.e. < M4), and therefore short durations of the events, and the short event-station distances (i.e. < 120 km), such that we expect both the P- and S-arrivals to occur within it.

2.2 Data quality control and preprocessing

After data retrieval. we band-pass filter each waveform between 1 and 15 Hz, a frequency range that spans most of the energy release of the regional microseismicity (e.g. Waldhauser and Schaff, 2008). Next we check all the data for each individual station for changes in sample rate, resampling all the waveforms to the minimum sample rate during the operation time or 100 Hz, whichever is larger. We also check for gaps in the data – gaps less than 5 seconds in duration are filled with zeros; we discard waveforms with gaps greater than 5 seconds. Finally, we cut a window of 10 seconds duration starting at the catalog P-wave pick time to be used for waveform cross-correlation purposes.

3. Identifying repeating earthquake families

We use a multi-stage approach to detect potential RE families. First, we systematically cross-correlate waveforms from different earthquakes at common stations using a pairwise approach, and assemble groups of events with high cross-correlation coefficients (CCCs) into single station clusters. Next, we compare the results for groups of similar events at multiple stations, in order to obtain more robust, multi-station clusters. After these initial filtering steps, we then apply three additional detection steps to discriminate between events that have similar locations, and events that are truly repeating: i) hierarchical clustering on the basis of CCCs at multiple stations; ii) measuring differential S–P arrival times at multiple stations in order to estimate hypocentral separation; and iii) estimating relative hypocentral location using the HypoDD code.

3.1 Identifying high cross-correlation event clusters at each station

For each station in turn, we start by calculating the CCC for each pair of events within each applicable subregion, and grouping similar events together. We employ a new fast method,

SEC-C (Super Efficient Cross-Correlation; Shakibay Senobari et al., 2018, submitted to Seismological Research Letters) that accelerates the calculation by up to 2 times over other methods for pairwise similarity search, using a rapid calculation of the normalized CCC in the frequency domain. We group together events with high CCCs into clusters, setting a minimum CCC threshold of 0.9. Note that at this stage this threshold is designed to exclude highly dissimilar events, rather than definitively select repeating events.

3.2 Producing multi-station clusters

We next merge all the clusters for different stations if they share a single event to make multi-station clusters (MSCs) for each subregion. Each event pair in a MSC has a CCC of 0.9 or greater on at least one station. We then make a three dimensional matrix of CCC values for each MSC. This n × n × m matrix, where n is the number of events in the cluster and m is the number of stations, is populated with the CCCs for each event pair for all detecting stations for a single MSC. Note that not every event in a MSC was detected by every station; in those cases, the corresponding elements of the matrix are assigned a null value.

In the next step, we make a n × n matrix of averaged CCC values for each event pair from the n × n × m matrix for each MSC by taking the average for the six highest CCCs along the station dimension (m). If fewer than six stations detected an individual event pair, we take the average for all available detecting stations, so long as there are at least three. We call the resulting matrix the ‘average CCC matrix’ for a given MSC. Examples of waveforms from such a cluster are shown in Figure 3.

3.3 Identifying repeating earthquake candidates through hierarchical clustering

As explained above, relying on a high CCC threshold alone to detect REs can be problematic. Therefore we employ a RE selection method that makes use of hierarchical clustering of average CCCs for each event pair, and that takes the recurrence interval (i.e. regularity of repeat time) and similarity of magnitude into consideration. We use the hierarchical clustering algorithm *linkage* and the plotting routine *dendrogram* in MATLAB to produce dendrograms – tree diagrams showing the hierarchy of similarity between events in a cluster based on average CCC values – and plot them for each average CC matrix, using a GUI that also provides magnitude and event time information for each event cluster. Based on these plots, we classify event clusters (or subsets of events in those clusters) into four groups:

1. Periodic repeating earthquake candidates. These consist of three or more events with high average CCC (typically >0.9), quasi-periodic recurrence intervals, and similar magnitudes.

2. Nonperiodic repeating earthquake candidates. These consist of three or more events that do not have periodic recurrence, but have a high CCC (>0.9).

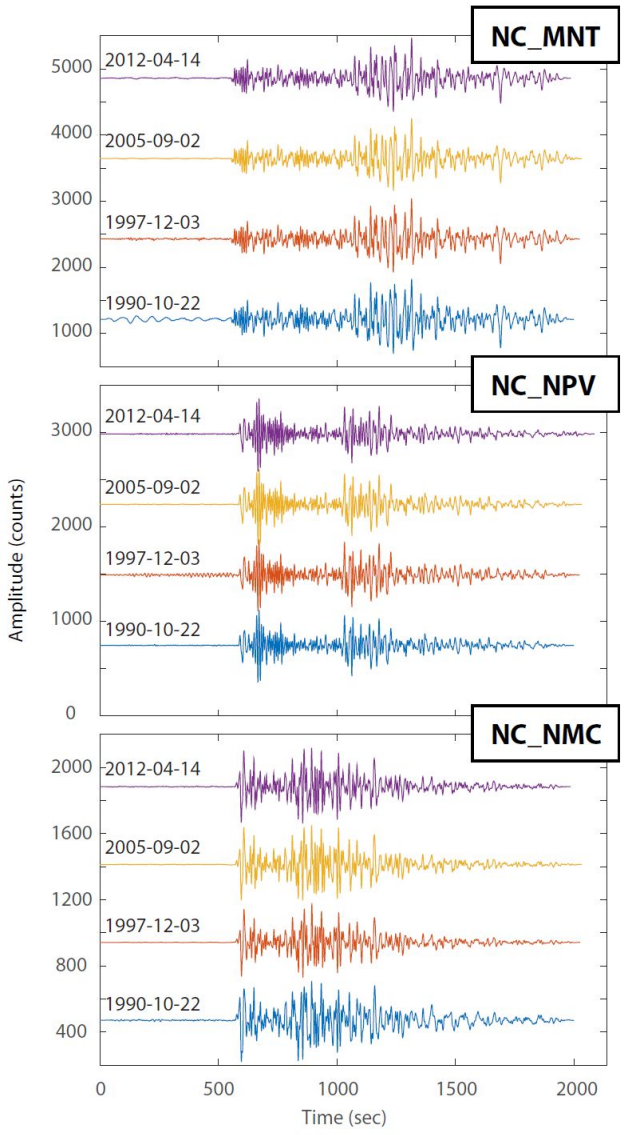

Figure 3 (left): Example waveforms of a repeating earthquake sequence from the Rodgers Creek fault (location: -122.7698°E, 38.5427°N, depth: 4.53 km). The events in the sequence have very high cross-correlation coefficients (>0.95) at all three stations shown (northern California stations MNT, NPV and NMC).

3. Repeating earthquake pair candidates. These are pairs of earthquakes with an interevent time of more than 3 yrs, and with high CC (>0.95). We do not know if these events are part of periodic or nonperiodic RE sequences in which some events were either not detected or have yet to occur, or if they are simply an earthquake source that repeated only once.

4. Nonrepeating earthquakes. These are groups of events that are similar, on the basis of high CCC, but not similar enough to be considered repeating earthquake sequences. Typically, we expect that these are earthquakes whose hypocentral locations are close in space, but not close enough that they have overlapping source radii.

Using these procedure we reduce false negative detections as we consider RE recurrence intervals, magnitude and CCC at the same time without defining a rigid CC threshold.

3.4 A location filter based on differential S–P times

In order to confirm that REs are coming from the same source region on a fault or not (i.e. to check if we get false positives from applying) we apply a second check on event similarity, based on similarity of location. Our approach to location filtering is based on measuring the differences in S–P times (Poupinet et al., 1984, Schaff et al., 2004, Chen et al., 2008, Uchida et al., 2007). S–P time is a function of source location and if we find identical S-P times for two events at stations with a variety of azimuths, we can say that the events originated at the same location. We can relax this constraint a little to include a maximum difference in S–P time that is

related to the estimated rupture size of an event, such that events with differential S–P times less than that maximum had significant overlap in their rupture areas.

In order to calculate precise differential S–P times for a pair of events we first select 1 s time windows around the P and S arrival phases in each waveform. If the S-wave pick was unclear, we used a 1 s time window centered on the peak of S-wave energy (Schaff et al., 2004). S–P travel time differences were estimated using the cross-spectral method (e.g. Poupinet et al., 1984). The delay times were estimated from the phases of cross spectra in a frequency band of 1–15 Hz with squared coherency of greater than ~0.9, at a precision of 0.001 s.

To use these differential time estimates in detection, we next must determine an appropriate threshold, based on the source dimension. We estimate this for each event pair assuming a back azimuth of 45° from the line connecting their epicenters, a Vp/Vs ratio of 1.72, the velocity model of Eberhart-Phillips (1986), the circular crack model of Eshelby (1957) and an assumed stress drop of 3.0 MPa. For a M2.5 event, a typical threshold time was ~0.008 s. An example, for a smaller event sequence is shown in Figure 4. We find that for more than 90 percent of our periodic, nonperiodic and single pair RE candidates the values for S-P difference are lower than the threshold for all the stations, consistent with their being repeating events.

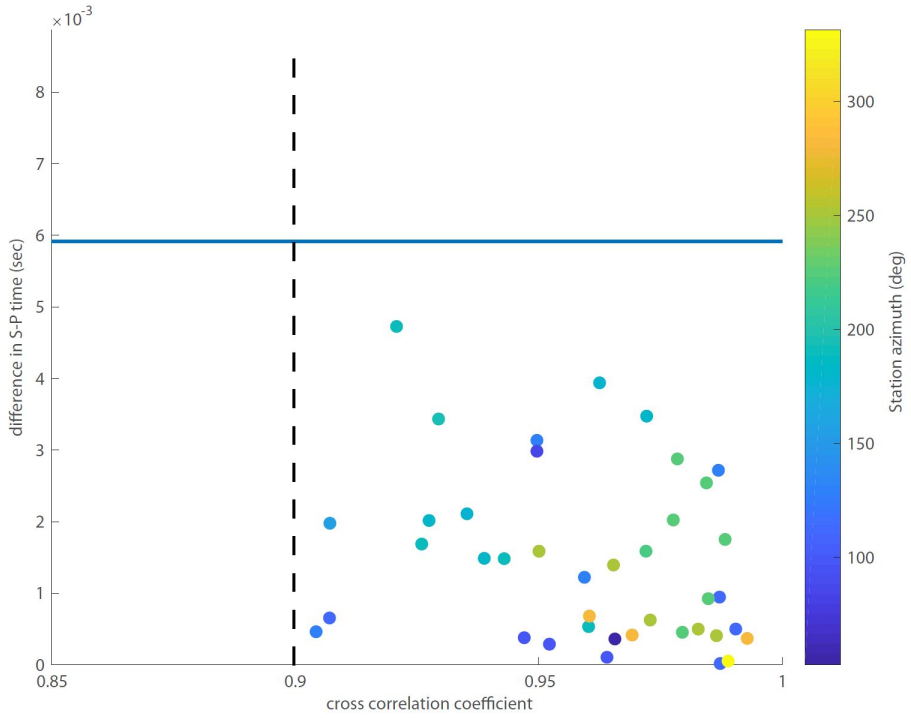

Figure 4: Repeating event filter based jointly upon cross-correlation coefficient and differential S–P time. Here, a threshold of 0.0059 s (for events with M~1.7; blue solid line) is used to exclude events that do not have 50% overlap of source radii, in addition to a cross-correlation coefficient cutoff of 0.9 (black dashed line).

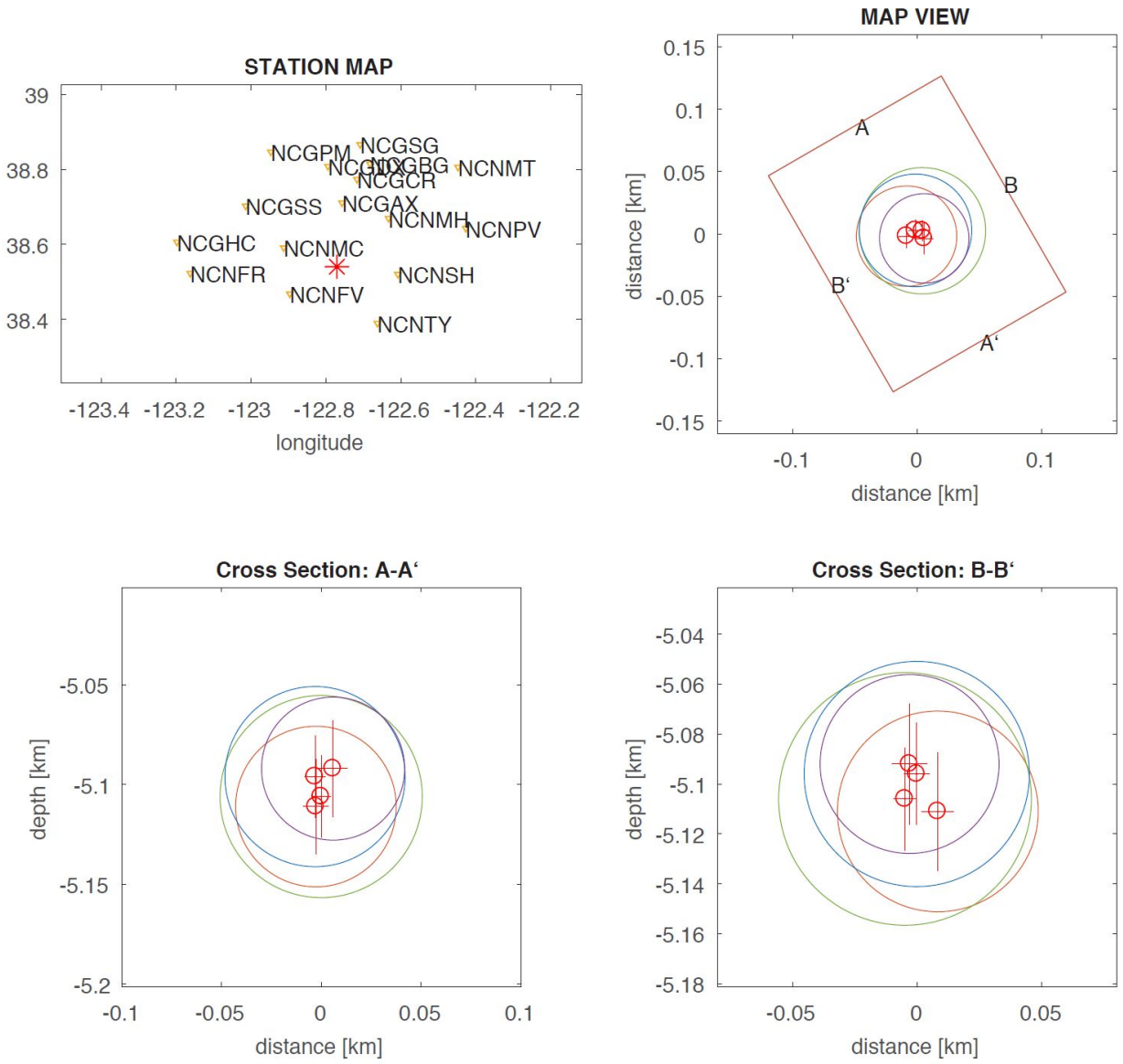

Figure 5: HypoDD location filtering for the Rodgers Creek fault event sequence whose waveforms are shown in Figure 3. Top left: stations used in the location process. Top right and bottom: Location comparisons in map view and cross-section. Colored circles indicate estimated source radii (color as Figure 3), red crosses indicate uncertainties in location. There is substantial overlap (>50%) between the events, indicating that they have a common source.

3.5 Confirming relative locations using HYPODD

As a final test on location similarity, we use the *HYPODD* code (Waldhauser and Ellsworth, 2000) and the methodology of Chen et al. (2008) to estimate precise relative locations for our candidate RE families. In this procedure we use the precise S-P times, as estimated above, as

well as an assumed velocity model. We confirmed our candidate families of events as 'true' REs if their sources areas overlap by 50 percent or more (e.g. Waldhauser and Ellsworth, 2000; Figure 5).

Using this approach, we confirm 191 repeating event groups in total: 54 periodic RE families, 42 nonperiodic RE families and 91 RE pairs (Figure 1). Almost all of the confirmed RE groups are located along major faults, as we shall discuss below.

.

4. Results

Our RE family and pair locations along the three major creeping faults in the region, the Maacama, Rodgers Creek and Bartlett Springs faults are plotted, along with double-difference relocated seismicity (Waldhauser and Schaff, 2008) in cross-section view in Figure 6. In the following sections we will describe these RE locations in greater detail.

4.1 Maacama fault

The Maacama fault shows the greatest amount of RE activity of the faults in the region. The along-strike cross-section (profile S1-T1; Figures 1 and 6), which includes both RE locations and the double-difference relocated seismicity shows that REs are pervasive along the fault. The maximum depth of REs increases, gradually, from south to north, from ~5 km near Cloverdale, to ~11 km NW of Willits. The majority of these RE families and pairs occur within a prominent band, or 'streak' in the relocated seismicity, which also increases in depth along-strike to the northwest. Such streaks of microearthquakes have been identified and associated with creep on other faults (e.g. Rubin et al., 1999).

The density of REs is greater than the average in a couple of areas along the Maacama fault – on the northern part of the fault in the vicinity of Willits (profiles A2-B2 and A3-B3; Figures 1 and 6) and on the southernmost part of the fault, extending NW from Cloverdale (profiles A5-B5, A6-B6 and A7-B7; Figures 1 and 4). In these locations, REs are present at shallower depths, as well as located along the 'microseismic streak' downdip. In both cases, RE locations are organized into two distinct individual down-dip trends in cross-section. We will describe these in more detail below.

At Willits, the deepest REs are aligned with the NE-dipping trend of microearthquakes that have previously been attributed to the ~60°-dipping main surface of the Maacama fault (e.g. Waldhauser and Ellsworth, 2000; profiles A1-B1 to A3-B3; Figure 6), suggesting that this structure could be creeping in the depth range 7–10 km. More intriguingly, the shallower REs in the area, located at depths of 1–5 km, are organized into a subvertical trend that projects to the surface ~5 km NE of the main Maacama surface trace, suggesting that there is a subvertical shallow splay fault at this location that may also be creeping (profile A3-B3; Figure 6).

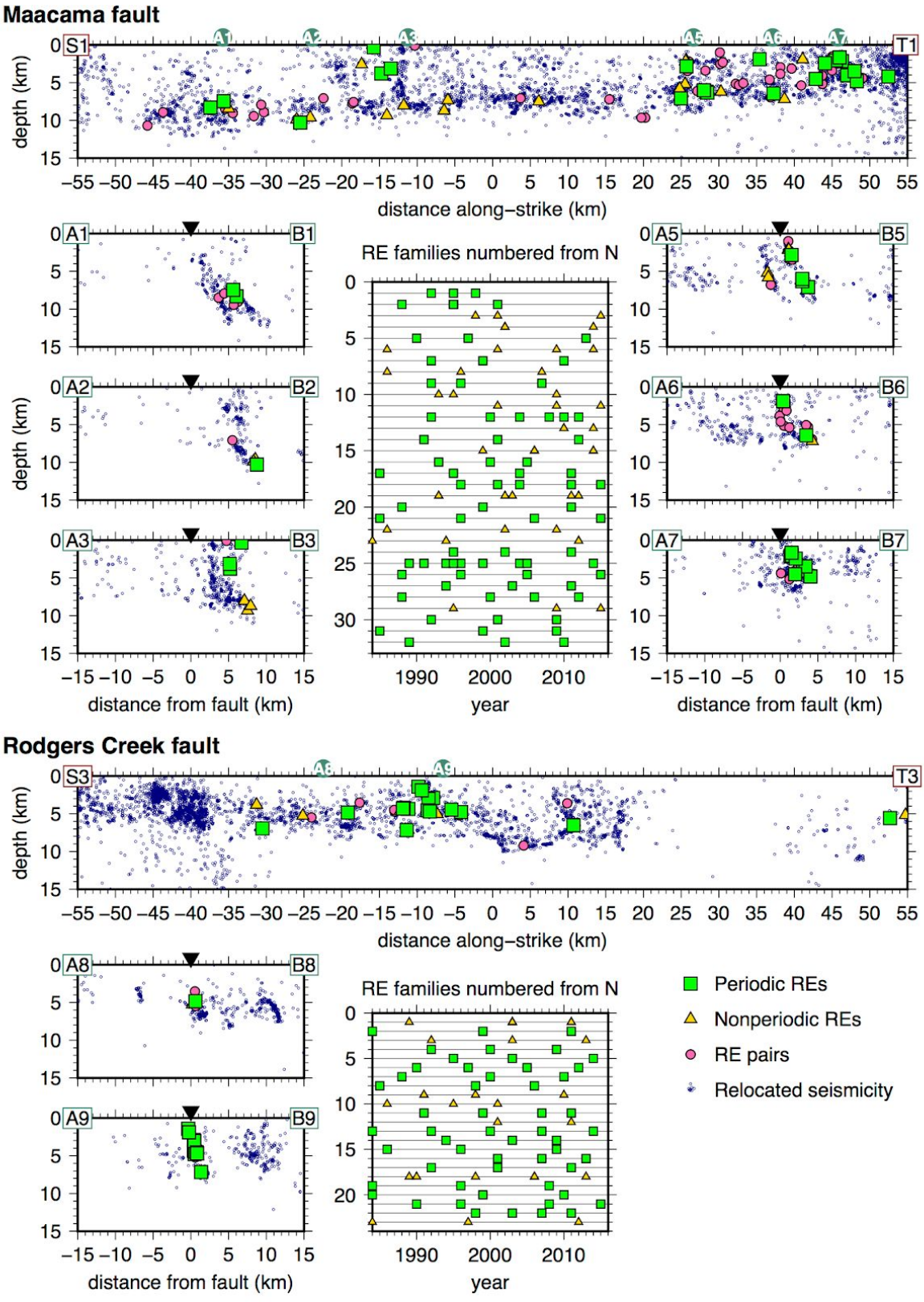

Figure 6: (Continued overleaf)

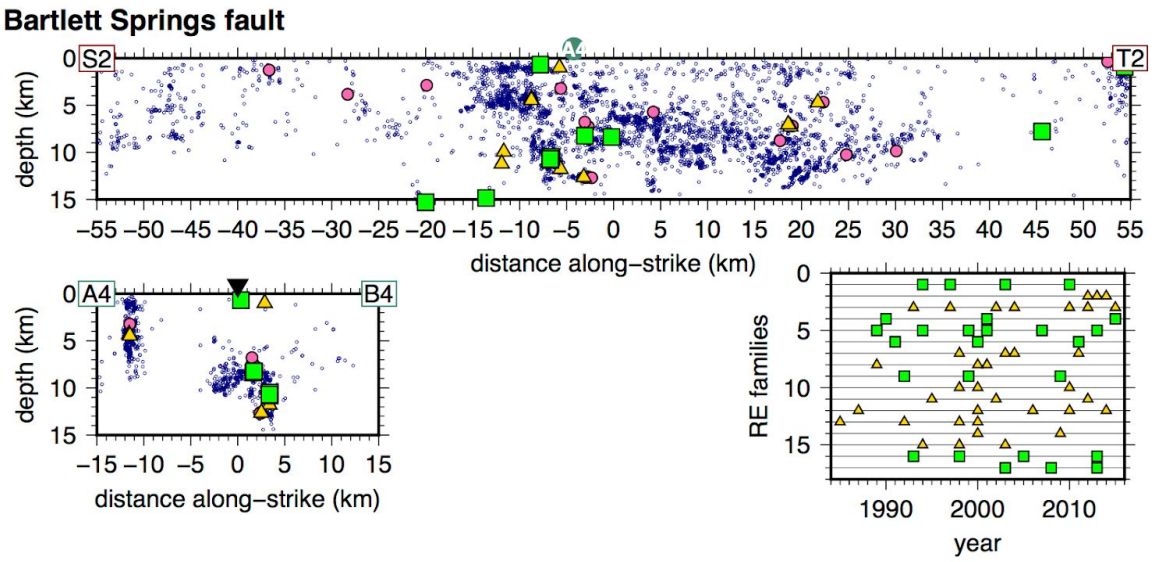

Figure 6: Repeating earthquakes (RE) along the major fault systems of the northern San Francisco Bay Area, plotted in cross-section and in time. Both fault-parallel (S-T) and fault perpendicular (A-B) profiles are shown; profile numbers and locations are given in Figure 1. We identify clusters of REs on the southern and northern Maacama fault, the central Rodgers Creek fault, and the central Bartlett Springs fault, suggesting that these sections of the fault are likely to be creeping. Time histories for RE families from each fault are arranged and numbered by latitude, from north to south. In general, we see no clear pattern of synchronicity between nearby RE families. More details provided in the main text. Symbols as for Figure 1.

This putative shallow subvertical splay at Willits projects to the location of a prominent Quaternary fault scarp on the east side of Little Lake Valley (the name given to the valley containing the city of Willits). This structure, which was covered as part of the GeoEarthScope Northern California LiDAR campaign in 2007 (data set downloadable from http://opentopo.sdsc.edu/datasetMetadata?otCollectionID=OT.052008.32610.1), is variously referred to as the 'East Willits fault' (e.g. Prentice et al., 2014) or the 'East Valley fault' (e.g. Woolace, 2005), and was recognized at least as early as the 1970s (e.g. Simon et al., 1978). Our results indicate, for the first time, to our knowledge, that this fault may be actively creeping.

The second area of structural complexity, in the vicinity of the city of Cloverdale, close to the southern end of the Maacama fault, shows two subparallel dipping structures picked out by RE locations and microseismicity in the 1-7 km depth range, approximately 2–3 km apart (profiles A5-B5 to A7-B7; Figures 1 and 6). The eastern of the two structures aligns with the mapped Holocene Maacama fault trace at the surface. It is not clear if the western structure has surface expression, however there are late Pleistocene and/or undated Quaternary structures mapped in the vicinity (USGS and CGS, 2006). To our knowledge, this is the first evidence that there are two currently active fault segments in this area, and that both are creeping at shallow depths.

4.2 Rodgers Creek fault

RE activity on the Rodgers Creek fault is almost entirely focused on the segment of the fault NW of the city of Santa Rosa (profiles A8-B8 and A9-B9; Figures 1 and 6). The same segment has been identified as creeping at the surface at rates of 2–6 mm/yr on the basis of persistent scatterer InSAR data (Funning et al., 2007; Jin and Funning, 2017); these estimates, based upon line-of-sight velocity offsets from fault-perpendicular profiles are only sensitive to creep within the top ~2 km of the fault. In contrast, REs within this segment are distributed across a depth range of 2–7 km (e.g. profile A9-B9; Figure 6), implying that the creep extends through those depths. The REs define a fault plane that dips steeply (~80°) to the NE.

4.3 Bartlett Springs fault

We identify REs across a wide range of depths (between 1 and 15 km) on the central Bartlett Springs fault, in a zone extending around 20 km NW of Lake Pillsbury (profiles S2-T2 and A4-B4; Figure 6). This is a location where both alinement array data and GPS data are consistent with surface creep at around 3–4 mm/yr (e.g. Murray et al., 2014; McFarland et al., 2016). The distribution of REs implies that creep could be occurring across the full seismogenic width of the fault along this zone. Elsewhere along the fault, the RE families and pairs are more diffuse, making it difficult to make definite statements on the distribution of creep in these areas.

4.4 Other faults

We identify two RE groups – a periodic RE family and a RE pair – on the West Napa fault, source fault of the 2014 M6.0 South Napa earthquake. The former, composed of three repeating events (in 1995, 2000 and 2005) is located on the Browns Valley segment of the fault, ~4 km NW of the northern end of the 2014 earthquake rupture zone (e.g. Floyd et al., 2016) and at 6 km depth. The 2014 earthquake showed abundant shallow aseismic afterslip, including slip on the southern portion of the Browns Valley segment, however no previous studies had identified any interseismic creep on the West Napa fault (e.g. Funning et al., 2007). The identification of repeating events on the West Napa fault suggests that portions of it may have been creeping prior to the 2014 event, albeit at a rate and depth that may not be detectable at the surface using geodetic data.

4.5 Temporal behavior

In order to identify any possible correlations in RE behavior in time, we plot the temporal history of the RE families along the three major faults in Figure 6, sorted by their positions along strike. We do not see any obvious synchroneity between sequences, implying that the are not triggered by nearby larger earthquakes (e.g. the 2014 South Napa event), or by transient aseismic slip on any of the major faults.

Acknowledgements

We thank Bob Nadeau for helpful suggestions at the start of this project, and Yan Zhu and Eamonn Keogh for useful discussions about similarity search and clustering.

References

Chen, K. H., R. M. Nadeau, and R.-J. Rau (2007), Towards a universal rule on the recurrence interval scaling of repeating earthquakes?, Geophys.Res. Lett., 34, L16308, doi:10.1029/2007GL030554.

Chen, K. H., Nadeau, R. M., and Rau, R. J. (2008), Characteristic repeating microearthquakes on an arc-continent collision boundary - the Chihshang fault of eastern Taiwan, Earth Planet. Sci. Lett., 276, doi:10.1016/j.epsl.2008.09.021

Eberhart-Phillips, D. (1986), Three-dimensional velocity structure in northern California Coast Ranges from inversion of local earthquake arrival times, Bull. Seismol. Soc. Am., 76, 1025-1052

Ellsworth, W. L. and L. D. Dietz, Repeating earthquakes: characteristics and implications, Proc. of Workshop 46, the 7th U.S.-Japan Seminar on Earthquake prediction, U.S.Geol.Surv. Open-File Rept. 90-98, 226-245, 1990.

Eshelby, J. D. (1957), The determination of the elastic field of an ellipsoidal inclusion, and related problems, Proc. Roy. Soc., Ser. A, 241,376-391

Floyd, M. A., R. J. Walters, J. R. Elliott, G. J. Funning, J. L. Svarc, J. R. Murray, A. J. Hooper, Y. Larsen, P. Marinkovic, R. Bürgmann, I. A. Johanson, and T. J. Wright (2016), Rupture and afterslip of the 2014 South Napa earthquake reveal spatial variations in fault friction related to lithology, Geophys. Res. Lett., 43, 6808–6816, doi:10.1002/2016GL069428

Funning, G. J., Bürgmann, R., Ferretti, A., Novali, F. and Fumagalli, A. (2007), Creep on the Rodgers Creek fault, northern San Francisco Bay area from a 10 year PS-InSAR dataset, Geophys. Res. Lett., 34, L19306, doi:10.1029/2007GL030836

Harsh, P. W., Pampeyan, E. H. and Coakley, J. M. (1978), Slip on the Willits fault, California, Earthquake Notes, 49, 22.

Hudnut, K.W., Brocher, T.M., Prentice, C.S., Boatwright, J., Brooks, B.A., Aagaard, B.T., Blair, J.L., Fletcher, J.B., Erdem, J.E., Wicks, C.W., Murray, J.R., Pollitz, F.F., Langbein, J., Svarc, J., Schwartz, D.P., Ponti, D.J., Hecker, S., DeLong, S., Rosa, C., Jones, B., Lamb, R., Rosinski, A., McCrink, T.P., Dawson, T.E., Seitz, G., Rubin, R.S., Glennie, C., Hauser, D., Ericksen, T., Mardock, D., Hoirup, D.F., and Bray, J.D. (2014), Key recovery factors for the August 24, 2014, South Napa earthquake: U.S. Geological Survey Open-File Report 2014–1249, 51 p., http://dx.doi.org/10.3133/ofr20141249.

Jin, L..and G. J. Funning (2017), Testing the inference of creep on the northern Rodgers Creek fault, California, using ascending and descending persistent scatterer InSAR data, J. Geophys. Res. Solid Earth, 122, doi:10.1002/2016JB013535

Johanson, I. A., Fielding, E. J., Rolandone, F. and Bürgmann, R. (2006), Coseismic and postseismic

slip of the 2004 Parkfield earthquake from space-geodetic data, Bull. Seism. Soc. Am., 96, 269-282.

McFarland, F. S, Lienkaemper, J. J and Caskey, S. J. (2016), Data from Theodolite Measurements of Creep Rates on San Francisco Bay Region Faults, California, 1979-2014, USGS Open File Report 2009–1119, v. 1.8.

Murray, J. R., Minson, S. E. and Svarc, J. L. (2014), Slip rates and spatially variable creep on faults of the northern San Andreas system inferred through Bayesian inversion of Global Positioning System data, J. Geophys. Res. Solid Earth, 119, 6023–6047, doi:10.1002/2014JB010966.

Nadeau, R. M., and L. R. Johnson (1998), Seismological studies at Parkfield VI: Moment release rates and estimates of source parameters for small repeating earthquakes, Bull. Seism. Soc. Am., 88, 790–814.

Nadeau, R. M., and T. V. McEvilly (1999), Fault slip rates at depth from recurrence intervals of repeating microearthquakes, Science, 285, 718–721.

Nadeau, R. M., and T. V. McEvilly (2004), Periodic pulsing of characteristic microearthquakes on the San Andreas Fault, Science, 303, 220–222, doi:10.1126/science.1090353.

Poupinet, G., Ellsworth, W.L. & Frechet, J., 1984. Monitoring velocity vari- ations in the crust using earthquake doublets: an application to the Calav- eras fault, California, J. geophys. Res., 89 (B7), 5719–5731

Rubin, A.M., D. Gillard, and J.-L. Got (1999), Streaks of microearthquakes along creeping faults, Nature, 400, 635-641.

Simon, R. B., E. H. Pampeyan and C. W. Stover (1978), The Willits, California, Magnitude-4.8 Earthquake of November 22, 1977, U.S. Geological Survey Open File Report 78-1075, 26 pp.

U.S. Geological Survey and California Geological Survey (2006), Quaternary fault and fold database for the United States, accessed April 6th, 2017, from USGS web site: http//earthquake.usgs.gov/hazards/qfaults/.

Vidale, J. E., W. L. Ellsworth, A. Cole, and C. Marone (1994). Variations in rupture process with recurrence interval in a repeated small earthquake, Nature 368, 624–629.

Waldhauser F. and W.L. Ellsworth (2000), A double-difference earthquake location algorithm: Method and application to the northern Hayward fault, Bull. Seism. Soc. Am., 90, 1353-1368.

Waldhauser, F., and D.P. Schaff (2008), Large-scale cross-correlation based relocation of two decades of Northern California seismicity, J. Geophys. Res. , 113, B08311, doi:10.1029/2007JB005479.

Waldhauser, F. (2009), Near-Real-Time Double-Difference Event Location Using Long-Term Seismic Archives, with Application to Northern California, Bull. Seism. Soc. Am., 99, 2376-2748.

Woolace, A. C. (2005), Late Neogene And Quaternary Stratigraphy And Structure Of Little Lake Valley, Northern Coast Range, California, M. S. Thesis, Humboldt State University, Arcata, CA, 67 pp.

Publications arising from this work to date

Zhu, Y, Z Zimmerman, N Shakibay Senobari, C-C M Yeh, G Funning, A Mueen, P Brisk and E Keogh (2018), Exploiting a Novel Algorithm and GPUs to Break the Ten Quadrillion Pairwise Comparisons Barrier for Time Series Motifs and Joins, Knowledge and Information Systems, 54, 206-206, doi:10.1007/s10115-017-1138-x